Available online at www.sciencedirect.com
SCIENCE DIRECT®
International Journal of Heat and Mass Transfer 48 (2005) 4942–4952
International Journal of HEAT and MASS TRANSFER
www.elsevier.com/locate/ijhmt

Thermal boundary resistance of nanocomposites

Ravi Prasher *

Intel Corporation, CH5-157, 5000 W. Chandler Blvd, Chandler, AZ 85226, United States

Received 2 September 2004; received in revised form 10 January 2005
Available online 15 August 2005

Abstract

This paper develops the general framework for the calculation of thermal boundary resistance between a substrate and a composite. All the previous works on the modeling of thermal boundary resistance have only dealt with pure materials. Thermal boundary resistance is dependent on the phonon equilibrium intensity and the transmissivity of phonons across the interface. These quantities depend on the group velocity, phase velocity and density of states of phonons. Due to multiple and dependent scattering of phonons the group velocity, phase velocity and the density of states are modified in a composite. Modification of these quantities is more dominant for nanocomposites at low temperatures. Results for silicon/germanium nanocomposite show that thermal boundary resistance can be severely modified depending on the temperature and size of the particulates. Results also show that when the particle size becomes large, the thermal boundary resistance between the substrate and the composite is same as that between the substrate and the host matrix of the composite.

1. Introduction

Thermal boundary resistance (R_b) plays an important role in determining heat flow, both in cryogenic and room-temperature applications, such as very large scale integrated circuitry, superlattices, and superconductors [1,2]. Two of the most common models used to predict [1,2] R_b are acoustic mismatch model (AMM) and diffuse mismatch model (DMM). Review of all the relevant literature [1] on R_b indicates that all the theoretical as well as experimental work have been done for R_b between two pure materials [1–10]. The question which has not been addressed is: what is the R_b between a substrate and a composite material? Is R_b same as that between the substrate and the host matrix of the composite or does it get modified? This question becomes even more important due to the advent of nanotechnology as composites can be made by using nano to macroparticles at will.

Materials using nano and microparticles mixed in a host matrix are going to play very important roles in future thermal technologies. Some potential applications of nanoparticles for thermal technologies have already been demonstrated [11–13]. Khitun et al. [12] and Liu et al. [13] used spherical quantum dot structures to reduce the phonon thermal conductivity to increase the efficiency of thermoelectrics. These composites can be used as thermoelectric devices. Some other relevant potential applications include nanoparticles mixed in a liquid to enhance the conductivity of liquids [11]. Other class of nanocomposites is composites made from nanoporous (NP) materials [14–16]. In these composites, the

* Present address: Department of Mechanical and Aerospace Engineering, Arizona State University, United States. Tel.: +1 480 554 0593.
E-mail address: ravi.s.prasher@intel.com

0017-9310/$ - see front matter © 2005 Elsevier Ltd. All rights reserved.
doi:10.1016/j.ijheatmasstransfer.2005.04.034

Nomenclature

a	radius of the particles
A_{In}	imaginary part of A_n
A_n	coefficient in the scattered wave
A_{Rn}	real part of A_n
B_n	coefficient in the transmitted wave
C_{sca}	scattering cross-section
$D(\omega)$	density of states
E	emissive power of phonons
F	scattering function
$f(0)$	forward scattering amplitude
g	ratio of density of the particle and the host medium
h	ratio of the wave speed in the particle and the host medium
h_n	spherical Hankel function of first kind
I	phonon intensity
j_n	spherical Bessel function
k	wave vector
k_I	imaginary part of k
k_R	real part of k
N	number of particles per unit volume (also used as indices in various equations)
P	stress field
P_n	Legendre function
q	heat flux
r	radius vector
R_1	$R_1 = 1/(gh^2) - 1$
R_2	$R_2 = (g-1)/(2g+1)$
R_b	thermal boundary resistance
u_r	radial component of particle velocity
v	velocity
v_g	group velocity
x	size parameter (ka)

Greek symbols

α	transmissivity of phonons
ϕ	volume fraction of particles
φ	azimuthal angle
θ	polar angle
ω	frequency

Subscripts

C	composite
i	incident field
M	host medium
P	particle
s	scattered field
t	transmitted field

pores are of nanometer size. NP materials are used in variety of applications. They will play even bigger roles in future technologies and applications. NP silicon is used as insulating substrate for microsensor design [16]. NP silicon is also being intensively investigated as sensors due their luminescence properties [15]. In sensors where it is necessary to get high thermal insulation in order to obtain a large temperature variation in correspondence to a small amount of heat, NP materials can be used due to their small thermal conductivity [15,16]. Other demonstrated/potential applications include their use as thermoelectrics [14], opal structures [17,18], boiling surfaces in cryogenic applications [19], low-k dielectrics in microelectronics. Other applications of nano and microcomposites are their use as particle-laden thermal interface materials at both room and cryogenic temperatures [20–22]. Researchers have also proposed the use of nanocomposites [23,24] and nanoporous opal structures [25,26] to be used as super conductors. Other relevant examples include the flow of helium over sintered materials [27]. In all the applications mentioned above, the knowledge of R_b of the nanocomposites is very important.

When these nanocomposites come in contact with a substrate, the thermal boundary resistance between the composites and the substrate will become important. This situation is shown in Fig. 1 where a composite is in intimate contact with a substrate. The composite shown in Fig. 1 is made of germanium (Ge) particles in silicon (Si) as the host medium. This composite will be referred as Si/Ge composite in this paper and calculations have been performed for this composite. The substrate is made of Ge. This situation can arise for example if a nanocomposite based thermoelectric is deposited on top of a microprocessor chip or a nanoporous material is fabricated on top of a substrate. Therefore, it is very important to develop a theoretical framework for calculating R_b of composites. Note that effect of R_b between the particle and the base matrix has been thoroughly investigated in literature [20]. This paper deals with R_b between a composite and the substrate it is in contact with.

This paper develops the general framework for the calculation of thermal boundary resistance between a substrate and a composite made of spherical particles. Thermal boundary resistance is dependent on the phonon equilibrium intensity and the transmissivity of phonons across the interface. These quantities depend on the group velocity (v_g), phase velocity (v) and density of states of phonons $D(\omega)$. Due to multiple and dependent scattering of phonons the group velocity, phase velocity and the density of states get modified in a

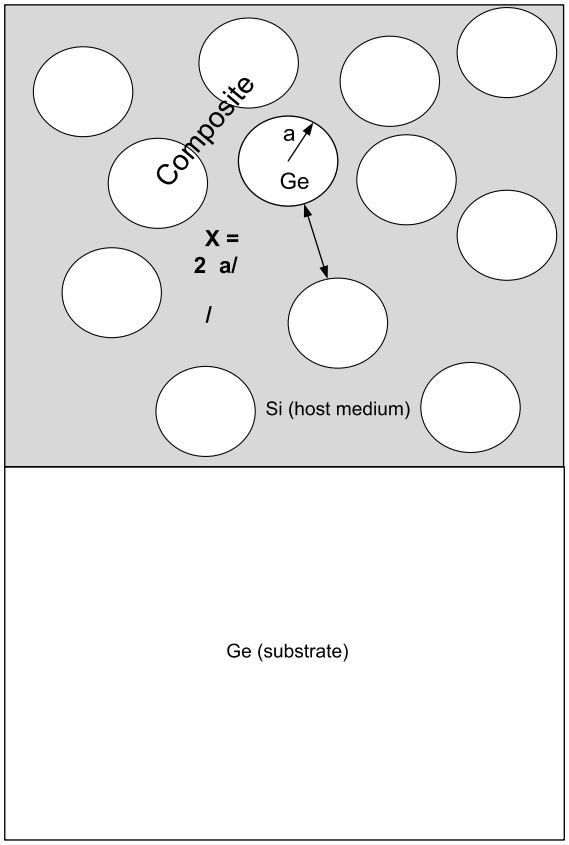

Fig. 1. Schematic to demonstrate the interface between a composite and a substrate. Composite considered in this paper is made of Si host and Ge particles. The substrate is assumed to be Ge.

composite. Results show that modification of these quantities is more dominant for nanocomposites at low temperatures.

2. Scattering of phonons by particles

Phonons are elastic waves. Elastic waves undergo mode conversion at the interface which leads to great mathematical complications in solving the scattering problem of elastic waves. The author has recently solved the scattering problem for all three polarizations of phonons [28–30] using the elastic wave equation. The focus of these papers was on single scattering and only on the calculation of single scattering cross-section, which is not at all important for the calculation of R_b. In this paper, we are dealing with effects of scattering of waves due to the presence of multiple boundaries on the dispersion relation of phonons. However in this paper acoustic wave equation without mode conversion is used primarily to reduce the mathematical complexity and to focus on the physics of the effects of multiple and dependent scattering on R_b. The elastic wave equation is a vector wave equation whereas the acoustic wave equation is a scalar wave equation. This also simplifies the mathematics a lot. It is also to be noted that all most all the work done on phonon scattering in literature has used the acoustic wave equation [12,13,31]. The acoustic wave equation is

$$\nabla^2 P = \frac{1}{v^2}\frac{\partial^2 P}{\partial t^2} \tag{1}$$

where P is the stress field and t is the time. Assuming sinusoidal waveform $P = p e^{-i\omega t}$ where ω is the frequency of the acoustic wave, Eq. (1) reduces to

$$(\nabla^2 + k^2)p = 0 \tag{2}$$

where $k = \omega/v$ is the wave vector. Since the particles are spherical in shape, Eq. (2) needs to be solved in spherical polar coordinates. To solve the scattering problem in the spherical polar coordinates the incident and transmitted plane waves need to be expanded in spherical harmonics [32]. In the spherical coordinates, the incident field (p_i), assuming unit amplitude is given as [32]

$$p_i = \sum_n^\infty i^n (2n+1) P_n(\cos\theta) j_n(k_M r) \tag{3}$$

where i is the imaginary number, $P_n(\cos\theta)$ the Legendre function, k_M the wave vector in the host medium, r the distance from the center of the scatterer as shown in Fig. 2 and j_n is the spherical Bessel function. Similarly, the transmitted field (p_t) is given as

$$p_t = \sum_n^\infty i^n B_n (2n+1) P_n(\cos\theta) j_n(k_P r) \tag{4}$$

where B_n is the undermined coefficient in the transmitted field and k_P is the wave vector in the particle. The scattered field (p_s) has to have a spherical waveform in the far field [28,30] as shown in Fig. 2. Therefore p_s is given as

$$p_s = \sum_n^\infty i^n A_n (2n+1) P_n(\cos\theta) h_n(k_M r) \tag{5}$$

where A_n is the undermined coefficient in the scattered field and h_n is the spherical Hankel function of first kind. In the far field ($r \to \infty$) it can be easily shown by using the asymptotic form of h_n that [33]

$$p_s = -\frac{\sum_{n=0}^\infty i A_n (2n+1) P_n(\cos\theta) e^{ik_M r}}{k_M r} \tag{6}$$

Eq. (6) shows that the scattered wave is a traveling spherical wave. Two boundary conditions are satisfied at the surface of the sphere ($r = a$): (a) the continuity of stress, (b) the continuity of the radial component of velocity, which is given by [32]

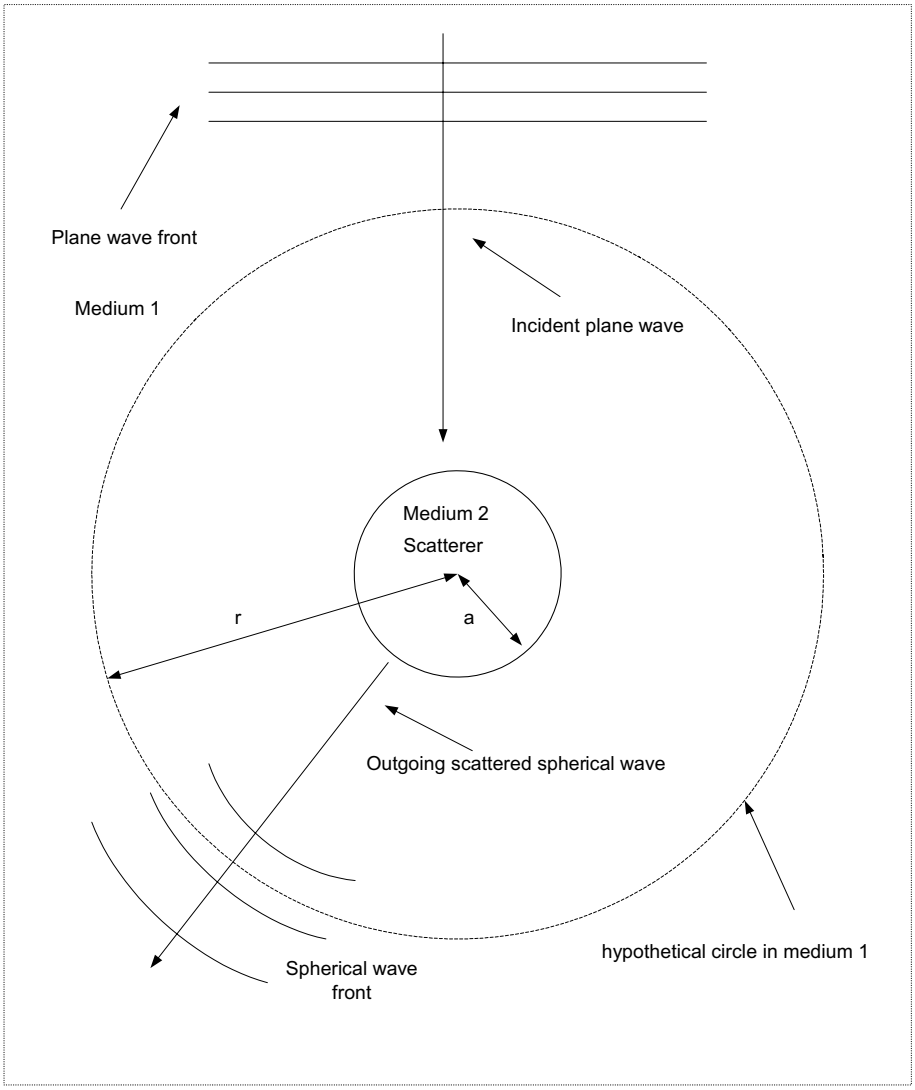

Fig. 2. Scattering a plane traveling wave by spherical scatterer.

$$u_r = \frac{-i}{\rho v}\frac{\partial p}{\partial (kr)} \tag{7}$$

where ρ is the density of the medium. Application of the two boundary conditions give [32]

$$A_n = -\frac{j_n'(k_P a) j_n(k_M a) - g h j_n(k_P a) j_n'(k_M a)}{j_n'(k_P a) h_n(k_M a) - g h j_n(k_P a) h_n'(k_M a)} \tag{8}$$

and

$$B_n = -\frac{g h\left[h_m'(k_M a) j_n(k_M a) - h_n(k_M a) j_n'(k_M a)\right]}{j_n'(k_P a) h_n(k_M a) - g h j_n(k_P a) h_n'(k_M a)} \tag{9}$$

where a is the radius of the particles and $g = \rho_P/\rho_M$ and $h = v_P/v_M$. The primes in Eqs. (8) and (9) represent differentiation with respect to the variables in the bracket.

In the Rayleigh regime ($k_M a \ll 1$ and $k_P a \ll 1$) it can shown that only first two terms in A_n are important and are given as [34]

$$A_0 = i\frac{R_1}{3}x^3, \quad A_1 = i\frac{R_2}{3}x^3 \tag{10}$$

where $x = k_M a$ is the size parameter, $R_1 = 1/(gh^2) - 1$ and $R_2 = (g-1)/(2g+1)$. For acoustic wave, it can be shown that the scattering function is [34]

$$F(\theta,\phi) = \sum_{m=0}^{\infty}\sum_{n=0}^{\infty} A_m \overline{A}_n (2m+1) \times (2n+1) p_n(\cos\theta) p_m(\cos\theta) \tag{11}$$

where $\overline{A}_n$ is the complex conjugate of A_n. The scattering cross-section (C_{sca}) of single a scatterer is given as [35]

$$C_{\mathrm{sca}} = \int_0^{\pi}\int_0^{2\pi} \frac{F(\theta,\phi)}{k_{\mathrm{M}}^2}\sin\theta\,\mathrm{d}\theta\,\mathrm{d}\phi = \frac{4\pi}{k_{\mathrm{M}}^2}\sum_{n=0}^{\infty}(2n+1)A_n\overline{A}_n \tag{12}$$

3. Modification of velocity of phonons due to multiple scattering: effective field approximation (EFA)

In this section effective wave properties of a composite are computed. In the presence of particles the effective wave vector (k_{C}) in the particulate media (composite) due to multiple scattering of the wave is given as [36]

$$k_{\mathrm{C}}^2 = k_{\mathrm{M}}^2 + 4\pi N f(0) \tag{13}$$

where N is the number of scatterer or particles per unit volume and $f(0)$ is the forward scattering amplitude. Realizing that $P_n(\cos 0) = 1$, $f(0)$ from Eq. (6) is

$$f(0) = -\frac{\mathrm{i}}{k_{\mathrm{M}}}\sum_{n=0}^{\infty}A_n(2n+1) \tag{14}$$

Separating A_n into real and imaginary part as $A_n = A_{\mathrm{R}n} + \mathrm{i}A_{\mathrm{I}n}$ and substituting Eq. (14) into Eq. (13) leads to

$$k_{\mathrm{C}}^2 = k_{\mathrm{M}}^2 + \frac{4\pi n}{k_{\mathrm{M}}}\sum_{n=0}^{\infty}A_{\mathrm{I}n}(2n+1) - \frac{\mathrm{i}4\pi n}{k_{\mathrm{M}}}\sum_{n=0}^{\infty}A_{\mathrm{R}n}(2n+1) \tag{15}$$

k_{C} can be separated into real and imaginary part as $k_{\mathrm{C}} = k_{\mathrm{R}} + \mathrm{i}k_{\mathrm{I}}$. k_{R} gives the effective phase velocity of the medium and k_{I} is related to the effective attenuation (β) of the wave in the medium as $\beta = 2k_{\mathrm{I}}$. k_{I} is needed in the calculation of the thermal conductivity of the composite if the particles serve as the scatterer of phonons [34]. k_{I} is not important in the calculation of R_{b}. Another interpretation of Eq. (15) is that k_{R} represents the coherent part of the wave and k_{I} represents the incoherent part of the wave. The scattering cross-section is also given as [37]

$$C_{\mathrm{sca}} = -\frac{4\pi}{k_{\mathrm{M}}}\sum_{n=0}^{\infty}A_{\mathrm{R}n}(2n+1) \tag{16}$$

Therefore Eq. (15) can be written as

$$\frac{k_{\mathrm{C}}^2}{k_{\mathrm{M}}^2} = 1 + \frac{4\pi N}{k_{\mathrm{M}}^3}\sum_{n=0}^{\infty}A_{\mathrm{I}n}(2n+1) + \frac{\mathrm{i}NC_{\mathrm{sca}}}{k_{\mathrm{M}}} \tag{17}$$

It can be shown that Eq. (17) gives the independent scattering results in the dilute scatterer limit by making a binomial expansion of Eq. (17)

$$\frac{k_{\mathrm{C}}}{k_{\mathrm{M}}} = 1 + \frac{2\pi N}{k_{\mathrm{M}}}\sum_{n=0}^{\infty}A_{\mathrm{I}n}(2n+1) + \frac{\mathrm{i}NC_{\mathrm{sca}}}{2k_{\mathrm{M}}} \tag{18}$$

Eq. (18) shows that $\beta = 2k_{\mathrm{I}} = NC_{\mathrm{sca}}$, giving the independent scattering result.

Eq. (17) can be written in terms of the volume fraction of the particles (ϕ) by substituting $N = 3\phi/(4\pi a^3)$ as

$$\frac{k^2}{k_{\mathrm{M}}^2} = 1 + \frac{3\phi}{x^3}\sum_{n=0}^{\infty}A_{\mathrm{I}n}(2n+1) + \frac{\mathrm{i}NC_{\mathrm{sca}}}{k_{\mathrm{M}}} \tag{19}$$

Eq. (19) can written as

$$\frac{k_{\mathrm{R}} + \mathrm{i}k_{\mathrm{I}}}{k_1} = \sqrt{Q + \mathrm{i}S} \tag{20}$$

where

$$Q = 1 + \frac{3\phi}{x^3}\sum_{n=0}^{\infty}A_{\mathrm{I}n}(2n+1) \tag{21}$$

$$S = \frac{n}{k_1}C_{\mathrm{sca}} \tag{22}$$

It can be easily shown [37] that

$$k_{\mathrm{R}} = k_{\mathrm{M}}\sqrt{1/2(L+S)} \tag{23}$$

$$k_{\mathrm{I}} = k_{\mathrm{M}}\sqrt{1/2(L-S)} \tag{24}$$

where

$$L = \sqrt{S^2 + Q^2} \tag{25}$$

Therefore

$$\frac{k_{\mathrm{I}}}{k_{\mathrm{R}}} = \sqrt{\frac{L-S}{L+S}} \tag{26}$$

Using Eq. (26) it can be shown that $k_{\mathrm{I}} \ll k_{\mathrm{R}}$. This was shown by the author for the case of photons [38]. Therefore k_{I}^2 can be neglected compared to other terms in Eq. (19). Eq. (19) can be written as

$$\frac{k_{\mathrm{R}}^2 + 2\mathrm{i}k_{\mathrm{R}}k_{\mathrm{I}}}{k_1^2} = 1 + \frac{3\phi}{x^3}\sum_{n=0}^{\infty}A_{\mathrm{I}n}(2n+1) + \frac{\mathrm{i}NC_{\mathrm{sca}}}{k_{\mathrm{M}}} \tag{27}$$

The velocity of phonon in the composite (v_{C}) can be written as $v_{\mathrm{C}} = k_{\mathrm{R}}/\omega$. Therefore from Eq. (27) the effective phonon phase velocity in the composite can be written as

$$v_{\mathrm{C}} = \frac{v_{\mathrm{M}}}{\left(1 + \frac{3\phi}{x^3}\sum_{n=0}^{\infty}(2n+1)A_{\mathrm{I}}\right)^{0.5}} \tag{28}$$

v_{g} is related to v_{C} by

$$v_{\mathrm{g}} = \frac{v_{\mathrm{C}}}{1 - \frac{\omega}{v_{\mathrm{C}}}\frac{\mathrm{d}v_{\mathrm{C}}}{\mathrm{d}\omega}} \tag{29}$$

Fig. 3 shows the variation of v_{C} for a composite made of germanium particle in silicon (called Si/Ge composite in the paper) for $\phi = 0.2$. In this paper velocity of all the three polarizations are assumed to be same and equal to the Debye speed. The physical properties if Si and Ge used for calculations are given in Table 1. Fig. 3 shows that in the geometric scattering (large values of x) regime

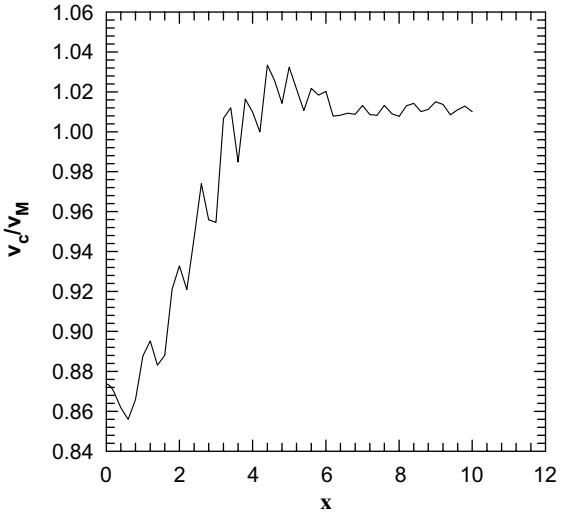

Fig. 3. v_C/v_M for different values of size parameter x.

Table 1
Physical properties of silicon and germanium used in calculations [24]

Material	Density (kg m^{-3})	Debye temperature (K)	Debye speed (m s^{-1})
Silicon (Si)	2330	645	5880
Germanium (Ge)	5320	374	3550

$v_C = v_M$, i.e. the effective velocity of phonons is same as the velocity of the host matrix. However at substantially large volume fractions v_C of macrocomposites can be different than v_M and more sophisticated approximations such as the coherent potential approximation [39] should be used to calculate v_C.

It is worth mentioning that researchers [40,41] have considered the modification of the dispersion relation of phonons due to geometry confinement in simple one dimensional nanowires. These studies have shown that v_g of nanowires can be significantly different from the v_g of the bulk material. The theoretical development on the modification of dispersion relation in composites as considered in this paper is inherently more complex than nanowires because of the presence of multiple boundaries due to multiple number of particles.

If the size of the particles is much smaller than the wavelength of the phonons either in the particle or in the medium then some of relations derived earlier can be simplified considerably. This regime is the Rayleigh scattering regime. In the Rayleigh scattering regime by using Eq. (10) v_C can be written as

$$v_C = \frac{v_M}{(1+\phi[R_1+3R_2])^{0.5}} \tag{30}$$

In the Rayleigh regime v_C is independent of frequency and the group velocity is same as the phase velocity of the phonons. Rayleigh regime basically means that the whole composite can be treated as a homogeneous material since the wavelength is much larger than the particle size. It is because of this reason, it can be seen from Eq. (30) that v_C is independent of the frequency. v_C is only a function of the volume fraction, density of the particle and the medium and the velocity of the phonons in the particle and the medium. The velocity of the phonons in any material is dependent on the modulus and the density of the medium. Therefore one can potentially define an effective modulus of the composite by using Eq. (30) as the density of the composite is given by, $\rho_C = (1-\phi)\rho_M + \phi\rho_P$.

One might be tempted to calculate the effective velocity of phonons in the composite by using some sort of rule of mixtures by using the velocity of phonons in the medium and the particle, however mixing formula cannot capture the physics of the problem. Fig. 3 shows that v_C is dependent on frequency and is same as v_M at higher frequency or smaller wavelength. Mixing formula cannot capture this frequency dependence. Eq. (8) shows that A_n depends not only v_P and v_M but also on ρ_P and ρ_M. Dependence on ρ_P and ρ_M has to be taken into account. In the Rayleigh regime where v_C is independent of frequency, v_C still depends on v_P and v_M and ρ_P and ρ_M. Therefore Eq. (30) can be considered as the simplest mixing formula to compute the velocity of phonons in the composite.

4. Modification of velocity of phonons due multiple and dependent scattering: quasi-crystalline approximation (QCA)

There are two pertinent length scales involved in the scattering of plane waves as shown in Fig. 1. First length scale is the size parameter x and second length scale is δ/λ where δ is the inter particle distance and λ is the wavelength of phonons. The value of δ/λ decides if the scattering is dependent or independent. In the dependent scattering regime a pair distribution function is used. Among various pair distribution functions Percus–Yevick (PY) [42] integral equation with appropriate particle-to-particle interactions is the best and can be used for larger volume fractions. Other pair distribution functions fail at volume fractions higher than 0.1. For a packed-sphere system the hard sphere potential applies [42]. Unfortunately for PY model analytical results can only be obtained for very small values of x i.e. in the Rayleigh regime. Drolen and Tien [42] have proposed that for $\delta/\lambda > 0.5$ dependent scattering effects are negligible. Since δ increases with increasing particle size therefore if the particle size is large then independent scattering will persist for larger volume fractions.

Lax [36] showed that Eq. (14) is valid only for small volume fractions i.e. Eq. (14) is not valid in the dependent scattering regime. Lax introduced a model called quasi-crystalline approximation (QCA) which deals with multiple and dependent scattering. Tsang et al. [43] have derived equations for QCA for both electromagnetic and acoustic waves using Percus–Yevick pair distribution function. Under QCA Eq. (14) modifies to

$$f(0) = -\frac{\mathrm{i}}{k_\mathrm{M}} \sum_{n=0}^{\infty} T_n A_n (2n+1) \tag{31}$$

where T_n is in Eq. (31) is due to the dependent scattering term and is dependent on the PY pair distribution function. This equation is substituted in Eq. (13) to derive v_C. v_C for QCA can be derived using the same methodology as EFA. However solution of QCA is very complicated compared to EFA for general values of x. For Rayleigh scattering analytical results were obtained by Tsang et al. [21]. In the Rayleigh regime v_C is given as

$$v_\mathrm{C} = \frac{v_\mathrm{M}}{\sqrt{\frac{(1+R_1\phi)(1+R_2\phi)}{1-2R_2\phi}}} \tag{32}$$

Fig. 4 shows the comparison between v_C calculated from EFA and QCA in the Rayleigh regime. Fig. 4 shows that dependent scattering does not affect v_C too much as both QCA and EFA are very close to each other. However dependent scattering affects the attenuation quite severely as shown by the author for both photons and phonons [14,18].

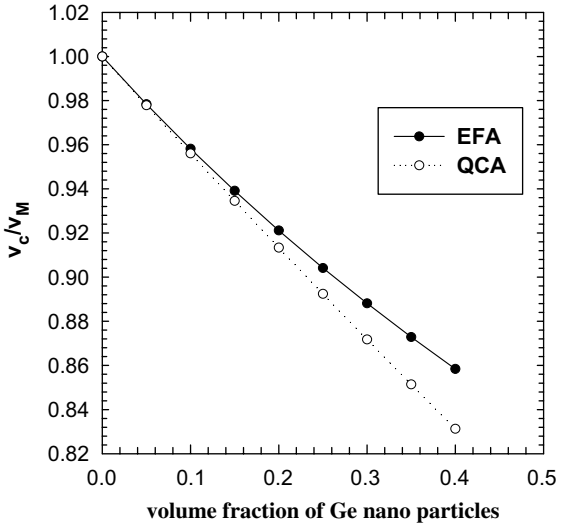

Fig. 4. $v_\mathrm{C}/v_\mathrm{M}$ in the Rayleigh regime for Ge (particles)/Si (host medium) nanocomposite.

5. Calculation of R_b

Basic formulations for the calculation of R_b are given in this section. The formulations for R_b are given in terms of phonon equilibrium intensity I^0 to make it consistent with the equation of phonon transport [44] and draw close analogy with radiation heat transport. I^0 is given by [45]

$$I_j^0(\omega) = \frac{1}{4\pi} v_{\mathrm{g},j} \frac{1}{\exp\left(\frac{\hbar\omega}{k_\mathrm{b}T}\right) - 1} \hbar\omega D_j(\omega) \tag{33}$$

where j denotes the polarization of phonon, $\hbar$ = Planck constant/2π and k_b the Boltzmann constant, T is the temperature. $I_j^0(\omega)$ is the spectral intensity within a unit small frequency interval centered around a single frequency ω. Analogous to black body radiation the emissive power of phonons which is the energy emitted per unit time within a unit small frequency interval centered around the frequency ω, per unit elemental surface area and into a unit elemental solid angle centered around the direction (θ, φ) can be defined as

$$E_j^0(\omega, \theta, \varphi) = I_j^0(\omega) \cos\theta \tag{34}$$

Total phonon emissive power can be written as

$$E_j = \int_0^{\omega_\mathrm{D}} \int_0^{\pi/2} \int_0^{2\pi} E_j^0(\omega, \theta, \varphi) \sin\theta \, \mathrm{d}\omega \, \mathrm{d}\theta \, \mathrm{d}\varphi \tag{35}$$

where ω_D is the Debye temperature. If two surfaces are in contact then the heat flux (q) from side 1 to 2 can be written as

$$\begin{aligned} q_{1-2} &= \int_0^{\omega_{\mathrm{D}<}} \int_0^{\pi/2} \int_0^{2\pi} E_j^0(\omega, \theta, \varphi) \alpha_{1-2}(j, \theta, \omega) \\ &\quad \times \sin\theta \, \mathrm{d}\omega \, \mathrm{d}\theta \, \mathrm{d}\varphi \\ &= \int_0^{\omega_{\mathrm{D}<}} \int_0^{\pi/2} \int_0^{2\pi} I_j^0(\omega) \alpha_{1-2}(j, \theta, \omega) \\ &\quad \times \cos\theta \sin\theta \, \mathrm{d}\omega \, \mathrm{d}\theta \, \mathrm{d}\varphi \end{aligned} \tag{36}$$

where α_{1-2} is the transmissivity of phonons from side 1 to 2 and $\omega_{\mathrm{D}<}$ is the smaller of the Debye frequency of the two sides. It can be easily shown that Eq. (36) is same as the familiar expression for q given in the literature [1]. $D(\omega)$ is given as

$$D(\omega) = \frac{k^2}{2\pi^2} \frac{\mathrm{d}k}{\mathrm{d}\omega} = \frac{\omega^2}{2\pi^2 v^2 v_\mathrm{g}} \tag{37}$$

$D(\omega)$ for the composite can be calculated using Eqs. (28) and (29). Due to multiple scattering of the phonons the Debye frequency and the Debye temperature (θ_D) are also modified as they are dependent on v. For the composite ω_D and θ_D are given as [46]

$$\omega_\mathrm{D} = \left(6\pi^2 \frac{N}{V}\right) v_\mathrm{C} \tag{38}$$

and

$$\theta_D = \frac{\hbar}{k_b}\left(6\pi^2\frac{N}{V}\right)v_C \tag{39}$$

where N is the number of primitive cells and V is the volume. Since v_C is frequency dependent except in the Rayleigh regime, therefore ω_D and θ_D are also frequency dependent. From Eq. (36) q due to all polarizations of phonons from side 1 to 2 is

$$q_{1-2} = \sum_j \frac{1}{4\pi^2}\int_0^{\omega_{D<}}\int_0^{\pi/2}\frac{1}{v_{1,j}^2} \times \frac{\hbar\omega^3}{\exp\left(\frac{\hbar\omega}{k_bT}-1\right)}\alpha_{1-2}(j,\theta,\omega) \times \sin\theta\cos\theta\,d\omega\,d\theta \tag{40}$$

Similarly q can be written for heat flux from side 2 to 1. Since the $v_C = v_M$ as shown in Fig. 3 for large values of x i.e. for macrocomposites where the wavelength is much smaller than the size of particles q, ω_D and θ_D are same as the host medium of the composite. For AMM [2]

$$\alpha_{1-2}(j) = \frac{4\frac{\rho_1 v_{1,j}}{\rho_2 v_{2,j}}\cos(\theta_1)\sqrt{1-\left[\frac{v_{2,j}}{v_{1,j}}\sin(\theta_1)\right]^2}}{\left[\cos(\theta_1)+\frac{\rho_1 v_{1,j}}{\rho_2 v_{2,j}}\sqrt{1-\left[\frac{v_{2,j}}{v_{1,j}}\sin(\theta_1)\right]^2}\right]^2} \tag{41}$$

where θ_1 is the angle of incidence of the phonons from side 1 to 2. Note that Eq. (41) is only valid of there is no mode conversion. Since in this paper phonons are treated as acoustic waves rather than elastic waves as mentioned earlier Eq. (41) can be used for all three polarization of the phonons. For DMM α is independent of angle of incidence and phonon polarization. α for DMM is given as

$$\alpha_{1-2} = \frac{\sum_j v_{j,2}^{-2}}{\sum_j v_{j,2}^{-2}+\sum_j v_{j,1}^{-2}} \tag{42}$$

If α and v are independent of ω then

$$q_{1-2} = \frac{1}{4\pi^2}\sum_j \frac{\Gamma_{1-2,j}}{v_{1,j}^2}\frac{(k_bT_1)^4}{\hbar^3} \times \int_0^{(\hbar\omega_{D<})/(k_bT_1)}\frac{u^3}{\exp(u)-1}\,du \tag{43}$$

where

$$\Gamma_{1-2,j} = \int_0^{\pi/2}\alpha_{1-2,j}(j,\theta)\cos\theta\sin\theta\,d\theta \tag{44}$$

At $T \ll$ Debye temperature [1]

$$q_{1-2} = \frac{\pi^2}{60}\sum_j \frac{\Gamma_{1-2,j}}{v_{1,j}^2}\frac{(k_bT_1)^4}{\hbar^3} \tag{45}$$

Therefore if α is independent of ω and the velocity of all polarizations are same as assumed in this paper then at low temperatures it can be easily shown that for AMM

$$R_b = \left(\frac{\pi^2}{5}\frac{\Gamma_{1-2}}{v_1^2}\frac{k_b^4}{\hbar^3}\right)^{-1}T^{-3} \tag{46}$$

and for DMM

$$R_b = \left(\frac{\pi^2}{10}\frac{1}{v_1^2+v_2^2}\frac{k_b^4}{\hbar^3}\right)^{-1}T^{-3} \tag{47}$$

Assuming that 1 represents the composite and 2 represents the substrate, the ratio of thermal boundary resistance of the composite (R_{b_C}) and the thermal boundary resistance of the medium (R_{b_M})

$$\frac{R_{b_C}}{R_{b_M}} = \left(\frac{v_C^2}{v_M^2}\right)\frac{\Gamma_{M-2}}{\Gamma_{C-2}} \tag{48}$$

for AMM and

$$\frac{R_{b_C}}{R_{b_M}} = \left(\frac{v_C^2+v_2^2}{v_M^2+v_2^2}\right) \tag{49}$$

for DMM. For Rayleigh scattering v_C is independent of frequency as shown by Eq. (30) and Rayleigh scattering results are valid at low temperatures. Therefore for Rayleigh scattering Eqs. (47) and (48) can be used to calculate R_b by using Eq. (30). Rayleigh regime is possible for nanocomposites at low temperatures due to small size of the particles and large wavelength of the phonons. Fig. 5 shows the ratio of integrated transmissivity (Γ) for the composite and pure Si for AMM for different volume fractions of Ge particles in the composite in the Rayleigh regime. Fig. 5 shows that Γ is not very different from that of pure Si. Ratio of R_b for Si/Ge nanocomposite and the R_b for pure Si are shown in Fig. 6 in

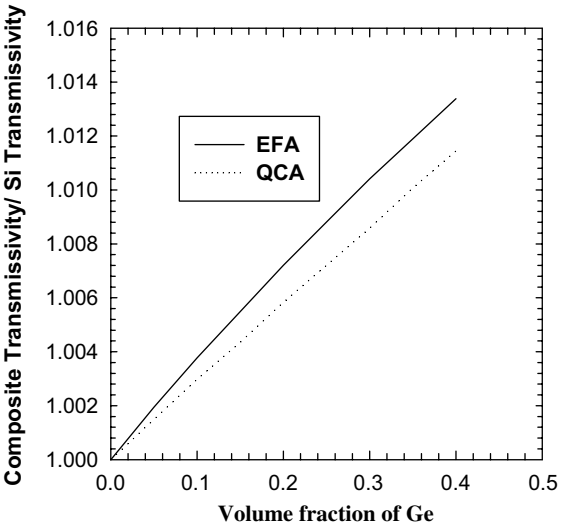

Fig. 5. Ratio of the AMM integrated transmissivity for the composite and pure Si.

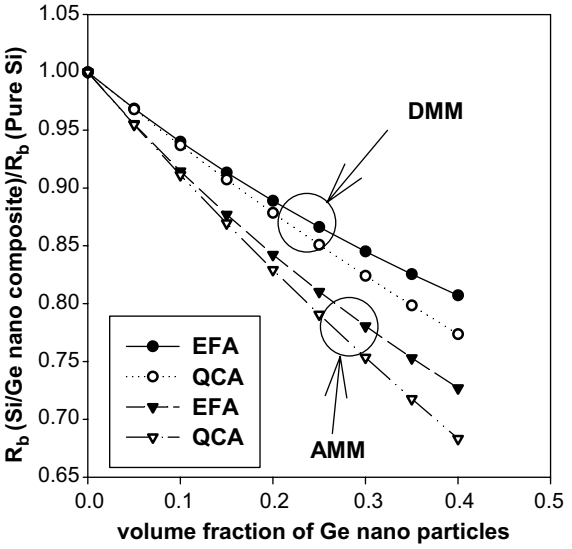

Fig. 6. Ratio of R_b in the Rayleigh regime of Ge (particles)/Si (host medium) nanocomposite and that of pure Si (Ge is the substrate).

the Rayleigh regime. Fig. 6 shows that R_b of Si/Ge nanocomposite is very different than the R_b of pure Si. Fig. 6 also shows that effect of dependent scattering (QCA) is not very dominant and R_b mainly gets modified due to the multiple scattering of phonons as R_b for both QCA and EFA are very close to each other for both AMM and DMM.

6. Discussion

The calculations were performed for Ge nanoparticles in Si, however the formulations can be used for other types of composites. As mentioned in Section 1, nanoporous composites hold a lot of promise for future applications. The velocity of the phonons in the Rayleigh regime can be significantly smaller for nanoporous materials. For example if nanoporous silicon is filled with Helium gas at cryogenic temperatures then assuming $\phi = 0.4$, we get, $v_c = 0.016 v_M$ in the Rayleigh regime. Similarly using DMM (Eq. (48)) $R_{b_C} = 0.267 R_{b_M}$ in the Rayleigh regime. These calculations show that R_b of nanoporous material filled with a gas will be significantly different than that of the medium. The calculations for both Si/Ge nanocomposite and nanoporous Si indicates the $v_C < v_M$ and hence $R_{b_C} < R_{b_M}$, however this trend is not universally true. This happened because the velocity of phonons in the Ge or He is smaller than the velocity of sound in Si. For example if we consider a composite made of Si nanoparticles in Ge matrix then using Eqs. (30) and (48) it can be easily shown that $v_C > v_M$ and $R_{b_C} > R_{b_M}$.

Another class of problems which can be potentially handled by the work developed in this paper is on the effects of grain boundaries on R_b, however this will not be very straightforward. Goodson [3,4] considered the impact of grain boundaries in diamond on thermal conduction normal to diamond-silicon boundaries. If an assessment of the impacts of grain boundaries on R_b has to be made then one needs to know the velocity of phonons in the grains as well as the density of the grains, which probably is not possible. Approximate upper bound analyses are normally made in assessing the impact of grain boundaries on thermal conductivity [4]. Similar approach can be taken to understand the impact of grain boundaries on R_b. One can make an upper bound estimate by assuming that the grain boundaries are rigid. Rigid boundaries mean that h and g in Eq. (8) becomes infinite. This makes $R_1 = -1$ and $R_2 = 0.5$. Therefore in the Rayleigh regime under the rigid boundary approximation $v_C = v_M/(1 + 0.5\phi)^{0.5}$.

7. Conclusions

Modeling of thermal boundary resistance of composites was presented in this paper. The main conclusions are:

(1) Due to multiple and dependent scattering of phonons R_b of composites get modified.
(2) Modification of R_b is more dominant for nanocomposites at low temperatures.
(3) R_b for macrocomposites are same as that of the host matrix for nominal volume fractions.
(4) Effects of multiple scattering are more dominant than dependent scattering on R_b.

Acknowledgements

The author gratefully acknowledges the support of the National Science Foundation, through a GOALI award (Award no. CTS-0353543), and the direct support provided by the Intel Corporation.

References

[1] E.T. Swartz, R.O. Pohl, Thermal boundary resistance, Rev. Modern Phys. 61 (3) (1989) 605–667.
[2] R.S. Prasher, P.E. Phelan, A scattering mediated acoustic mismatch model for the prediction of thermal boundary resistance, J. Heat Transfer 123 (1) (2001) 105–112.
[3] K.E. Goodson, O.W. Kading, M. Rosner, R. Zachai, Thermal conduction normal to diamond-silicon boundaries, Appl. Phys. Lett. 66 (23) (1995) 3134–3136.

[4] K.E. Goodson, O.W. Kading, M. Rosner, R. Zachai, Experimental investigation of thermal conduction normal to diamond-silicon boundaries, J. Appl. Phys. 77 (4) (1995) 1385–1392.
[5] E.T. Swartz, R.O. Pohl, Thermal resistance at interfaces, Appl. Phys. Lett. 51 (26) (1987) 2200–2202.
[6] C.W. Bettenhausen, W.C. Bowie, M.R. Geller, Elasticity theory connection rules for epitaxial interfaces, Phys. Rev. B 68 (2003) 035431-1–035431-7.
[7] D.G. Cahill, W.K. Ford, K.E. Goodson, G.D. Mahan, A. Majumdar, H.J. Maris, R. Merlin, S.R. Phillpot, Nanoscale thermal transport, J. Appl. Phys. 93 (2) (2003) 793–818.
[8] R.J. Stoner, H.J. Maris, Kapitza conductance and heat flow between solids at temperatures from 50 to 300 K, Phys. Rev. B 48 (22) (1993) 16373–16387.
[9] T. Zeng, G. Chen, Phonon heat conduction in thin films: impacts of thermal boundary resistance and internal heat generation, J. Heat Transfer 123 (2) (2001) 340–347.
[10] S. Pettersson, G.D. Mahan, Theory of the thermal boundary resistance between dissimilar lattices, Phys. Rev. B 42 (12) (1990) 7386–7390.
[11] P. Keblisnki, S.R. Phillpot, S.U.S. Choi, J.A. Eastman, Mechanisms of heat flow in suspensions of nano-sized particles (nanofluids), Int. J. Heat Mass Transfer 45 (2002) 855–863.
[12] A. Khitun, A. Balandin, J.L. Liu, K.L. Wang, In-plane thermal conductivity of a quantum-dot superlattice, J. Appl. Phys. 88 (2) (2000) 696–699.
[13] J.L. Liu, A. Khitun, K.L. Wang, W.L. Liu, G. Chen, Q.H. Xie, S.G. Thomas, Cross-plane thermal conductivity of self-assembled Ge quantum dot superlattices, Phys. Rev. B (67) (2003) 165333-1–165333-6.
[14] D.W. Song, W.-N. Shen, B. Dunn, C.D. Moore, M.S. Goorsky, T. Radetic, R. Gronsky, G. Chen, Thermal conductivity of nanoporous bismuth thin films, Appl. Phys. Lett. 84 (11) (2004) 1883–1885.
[15] G. Gesele, J. Linsmeier, V. Drach, J. Fricke, R. Arens-Fischer, Temperature-dependent thermal conductivity of porous silicon, J. Phys. D: Appl. Phys. 30 (1997) 2911–2916.
[16] G. Benedetto, L. Boaring, N. Brunetto, A. Rossi, R. Spagnolo, G. Amato, Thermal properties of porous silicon layers, Philos. Mag. 76 (3) (1997) 383–393.
[17] R.H. Baughman, A.A. Zakhidov, I.I. Khayrullin, I.A. Udod, C. Chiu, G.U. Sumanasekera, L. Grigorian, P.C. Eklund, V. Browning, A. Ehrlich, Nanustructured thermoelectrics based on periodic composites from opals ad opal replicas: I. Bi-infiltrated Opals, in: 17th International Conference on Thermoelectrics, 1998, pp. 288–293.
[18] J.O. Safo, G.D. Mahan, Transport in opal structures, in: 18th International Conference on Thermoelectrics, 1999, pp. 626–629.
[19] T.M. Kuzay, Cryogenic cooling of X-ray crystals using a porous matrix, Rev. Sci. Instrum. 63 (1) (1992) 468–472.
[20] R.S. Prasher, J. Shipley, S. Prstic, P. Koning, J.-L. Wang, Thermal resistance of particle laden polymeric thermal interface material, J. Heat Transfer 125 (6) (2003) 1170–1176.
[21] F. Rondeaux, Ph. Bredy, J.M. Rey, Thermal conductivity measurement of epoxy systems at low temperature, Proc. Int. Cryog. Mater. Conf.—ICMC 48 (2002) 197–203.
[22] M. Jackel, Thermal properties of polymer/particle composites at low temperatures, Cryogenics 35 (11) (1995) 713–716.
[23] X. Wan, Y. Sun, W. Song, K. Wang, L. Jiang, J. Du, Enhanced flux pinning of Bi-2223/Ag tapes with Nano-MgO particle addition, Physica C 307 (1998) 46–50.
[24] X.F. Rui, J. Chen, X. Chen, W. Guo, H. Zhang, Doping effect of nano-alumina on MgB_2, Physica C 412–414 (2004) 312–315.
[25] V.N. Bogomolov, L.S. Parfen'eva, I.A. Smirnov, H. Misiorek, A. Jezowski, A.I. Krivhikov, B.I. Verkin, Low-temperature heat capacity and heat conductivity of single-crystal synthetic opals, Phys. Solid State 43 (1) (2001) 190–193.
[26] E.V. Charnaya, C. Tien, K.J. Lin, C.S. Wur, Y.A. Kumzerov, Superconductivity of gallium in various confined geometries, Phys. Rev. B 58 (1) (1998) 467–472.
[27] D.J. Cousins, A.M. Guenault, G.R. Pickett, P. Thibault, R.P. Turner, E.N. Smith, C. Bauerle, Y.M. Bunkov, S.N. Fisher, H. Godfrn, A geometry dependent thermal resistance between a saturated He^3 and He^4 solution and sintered silver powder, J. Low Temp. Phys. 101 (1–2) (1995) 259–264.
[28] R.S. Prasher, Mie scattering theory of phonon transport in particulate media, J. Heat Transfer 126 (2004) 793–804.
[29] R. Prasher, Thermal transport cross section and phase function of longitudinal phonons for scattering by nano and micro particles, J. Appl. Phys. 96 (9) (2004) 5202–5212.
[30] R. Prasher, Thermal transport due to transverse phonons in nano and micro particulate media, J. Appl. Phys. 97 (2005) 064313-1-8.
[31] J.M. Ziman, Electrons and Phonons, Oxford Press, London, 1996.
[32] C. Feuillade, C.S. Clay, Anderson (1950) revisited, J. Acoust. Soc. Am. 106 (2) (1999) 553–564.
[33] G.B. Arfken, H.J. Weber, Mathematical Methods for Physicists, Academic Press, San Diego, 1995.
[34] R. Prasher, Thermal transport due to phonons in nano-particulate media, in: The multiple and dependent elastic scattering regime, Paper no. HT2005-72045, Proceedings of HT2005, 2005 ASME Summer Heat Transfer Conference, 17–22 July 2005, San Francisco, California, USA.
[35] V.C. Anderson, Sound scattering from fluid sphere, J. Acoust. Soc. Am. 22 (1950) 426–431.
[36] M. Lax, Multiple scattering of waves, Rev. Modern Phys. 23 (4) (1951) 287–310.
[37] G.C. Gaunard, W. Wertman, Comparison of effective medium theories for inhomogeneous continua, J. Acoust. Soc. Am. 85 (2) (1989) 541–554.
[38] R. Prasher, Modification of Planck black body emissive power and intensity in particulate media due to multiple and dependent scattering, J. Heat Transfer, in press.
[39] P. Sheng, Introduction to Wave Scattering, Localization and Mesoscopic Phenomena, Academic Press, San Diego, 1995.
[40] J. Zou, A. Balandin, Phonon heat conduction in a semiconductor nanowire, J. Appl. Phys. 89 (5) (2001) 2932–2938.
[41] X. Lu, J.H. Chu, W.Z. Shen, Modification of the lattice thermal conductivity in semiconductor rectangular nanowires, J. Appl. Phys. 93 (2) (2003) 1219–1229.

[42] B.L. Drolen, C.L. Tien, Independent and dependent scattering in packed sphere systems, J. Thermophys. 1 (1) (1987) 63–68.
[43] L. Tsang, J.A. Kong, T. Habashy, Multiple scattering of acoustic waves by random distribution of discrete spherical scatterers with quasicrystalline and Percus–Yevick approximation, J. Acoust. Soc. Am. 71 (3) (1982) 552–558.
[44] R.S. Prasher, Phonon transport in anisotropic scattering particulate media, J. Heat Transfer 125 (6) (2003) 1156–1162.
[45] A. Majumdar, Microscale heat conduction in dielectric thin films, Journal of Heat Transfer 115 (1) (1993) 7–16.
[46] C. Kittel, Introduction to Solid State Physics, sixth ed., John Wiley & Sons, Singapore, 1986.